Nucleic Acids Research, 1998, Vol. 26, No. 11 **2797–2802**

The influence of fluorescent dye structure on the electrophoretic mobility of end-labeled DNA

Oanh Tu, Tim Knott[1], Michele Marsh, Kate Bechtol, Dennis Harris, David Barker and John Bashkin*

Molecular Dynamics, Sunnyvale, CA 94086, USA and [1]Amersham International, Amersham, UK

Received January 29, 1998; Revised and Accepted April 16, 1998

ABSTRACT

Over the past 10 years, fluorescent end-labeling of DNA fragments has evolved into the preferred method of DNA detection for a wide variety of applications, including DNA sequencing and PCR fragment analysis. One of the advantages inherent in fluorescent detection methods is the ability to perform multi-color analyses. Unfortunately, labeling DNA fragments with different fluorescent tags generally induces disparate relative electrophoretic mobilities for the fragments. Mobility-shift corrections must therefore be applied to the electrophoretic data to compensate for these effects. These corrections may lead to increased errors in the estimation of DNA fragment sizes and reduced confidence in DNA sequence information. Here, we present a systematic study of the relationship between dye structure and the resultant electrophoretic mobility of end-labeled DNA fragments. We have used a cyanine dye family as a paradigm and high-resolution capillary array electrophoresis (CAE) as the instrumentation platform. Our goals are to develop a general understanding of the effects of dyes on DNA electrophoretic mobility and to synthesize a family of DNA end-labels that impart identically matched mobility influences on DNA fragments. Such matched sets could be used in DNA sequencing and fragment sizing applications on capillary electrophoresis instrumentation.

INTRODUCTION

With the expanding use of multi-color fluorescent detection as a routine method for DNA analysis, a number of advances have occurred in dye technology (1–8). One aspect of this is the extension of excitation wavelengths from the visible-blue region (2–6) to the infra-red (9), taking advantage of the lower fluorescent backgrounds obtained at longer excitation wavelengths. Fluorescence energy transfer (ET) has also been exploited to generate dyes with increased fluorescent yields and long Stokes shifts (3–8).

Efforts have been made to develop families of dyes that induce minimal relative mobility shifts between labeled DNA fragments (3–8). In general, this has been accomplished by adjusting the structure of the dye–DNA linker (6) or, in the case of ET dyes, by adjusting the physical separation between donor and acceptor dyes. For the ET dyes, the efficiency of the energy transfer was initially sacrificed to achieve a minimal spread in DNA mobilities (3–8).

During our development of capillary array electrophoresis (CAE) for high-throughput DNA analysis (10–12), we found that mobility shifts may be much more apparent with CAE than with traditional slab gel electrophoresis (12) and that dyes exhibiting matched mobilities in a slab gel format may still display significant relative shifts in CAE. We have, therefore, undertaken a systematic study of the relationship between dye structure and labeled-DNA electrophoretic mobility and have analyzed the mobility of the series using CAE. We chose as a dye family the cyanine group developed by Waggoner and colleagues for DNA analysis (13–16). This series affords both the potential of tremendous synthetic control and the ability to generate structurally similar compounds that fluoresce over a broad wavelength range.

MATERIALS AND METHODS

The 48-capillary array electrophoresis instrument has been described previously (10), except that a 10 mW HeNe laser (633 nm, Uniphase, San Jose, CA) was used in place of the 20 mW Ar^+ (488 nm), and the instrument was fitted with the high pressure anode manifold described previously (11). Briefly, the laser is focused onto the capillary array plane by a microscope objective (Nikon 40× ELWD, Technical Instruments, Corp., San Francisco, CA) which is mounted to a translation stage (stage and controllers were purchased from Daedel, Harrison City, PA). The fluorescent light is collected by the same objective, passed back through a series of optical elements (Omega Optical, Battleboro, VT) and focused onto two confocal spatial filters placed in front of two photomultiplier tube (PMT) housings (Hamamatsu R1477-05, Hamamatsu Photonics, Bridgewater, NJ). Each PMT housing contains a PMT and a longpass or bandpass filter.

The electrophoresis voltage was supplied by a 20 kV power supply (Bertan, Hicksville, NY). Data from the photomultipliers were read into a 12 bit DAS48PGA board, while capillary current information was collected by a 12 bit DAS16/330 board, both from ComputerBoards, Inc. (Mansfield, MA). Images and current data were analyzed with ArrayQuant™, a software package developed in-house that runs under the WindowsNT® operating system.

The 48 capillaries (200 µm OD, 75µm ID, Polymicro Technologies, Phoenix, AZ) were fabricated into a 16-capillary array as described previously (11), with a detection length of 40 cm and a total length of 65 cm. To eliminate electroendosmotic forces, the interior glass surface was coated with polyacrylamide using the procedure either of Hjertén (17) or Cobb (18).

*To whom correspondence should be addressed. Tel: +1 408 737 3130; Fax: +1 408 773 8343; Email: jbashkin@mdyn.com

The HEC sieving buffer was prepared as described previously (11). All experiments used a 1.5% HEC solution, except as noted in the text. For this matrix, a 100 ml solution was prepared by dissolving 1.88 g hydroxyethylcellulose (HEC, 140 000–160 000 MW, Polysciences, Warrington, PA) and 45 g urea (Aldrich Chemical, Milwaukee, WI) in 63.4 ml water. This solution was stirred overnight with 1 g Amberlite™ MB-1 ion-exchange resin (Mallinkrodt, Paris, KY). The solution was then transferred to 25 ml tubes and centrifuged in a table-top centrifuge for 30 min. The matrix was decanted off the pelleted resin. To 80 ml of the purified matrix, 10 ml of 10× TBE (1× TBE: 89 mM Tris, 89 mM boric acid, 2 mM EDTA, pH 8.0) and 10 ml of deionized formamide were added. The final solution was stirred for 15 min then degassed under vacuum for 0.5 h. For a 1.25% HEC buffer, the same procedure was followed, except 1.56 g of HEC were used.

DNA T-termination sequencing samples were prepared using M13mp18 and Labstation Automated ThermoSequenase™ sequencing kits from Amersham Corporation (Arlington Heights, IL). Briefly, reactions were assembled and subjected to 30 cycles of a three-temperature protocol (95°C for 30 s, 56°C for 30 s, 72°C for 30 s). The amount of primer varied (0.5–2 pmol) depending on the spectral properties of the cyanine dye derivatives. The thermal cycler was a DNA Engine Tetrad from MJ Research (Watertown, MA). Reactions were precipitated, washed with 70% EtOH and dried in a SpeedVac concentrator (Savant Instruments, Farmingdale, NY). Samples were then denatured in 3 µl 80% deionized formamide (Gibco BRL, Gaithersburg, MD) by heating at 85°C for 5 min and placed on ice. Electrokinetic injections were done for 15 s at 185 V/cm, and electrophoresis was continued at 185 V/cm. Runs were performed at 28°C except for the thermodynamic studies, which were performed at 34 and 42°C.

Dyes were synthesized by Biological Detection Systems (Pittsburgh, PA) and Amersham using variations on published procedures and were provided as labeled M13 –40 primers (5′-Dye-GTTTTCCCAGTCACGAC-3′). Dyes were purified by HPLC prior to end-labeling. Conjugation of the dyes to the primers was accomplished through standard NHS-ester procedures, and the labeled primers were purified by HPLC.

RESULTS AND DISCUSSION

The Cy5™/Cy5.5™ cyanine family of dyes (CY5s/CY5.5s) is excitable at 633 nm. The high degree of subtle structural variation possible with these dyes allowed us to evaluate the effects on DNA mobility of net dye charge, charge placement, peripheral structure and linkage-arm placement. We also tested the effects of conformational flexibility between the two halves of the cyanine dye structure by examining a series of squaric acid derivatives of CY5 dyes (SQ5s). In all, six different CY5 dyes, ten SQ5s and eight CY5.5s were evaluated. The structures for the entire set are shown in Figure 1.

We measured the relative migration patterns of pairs of DNA's labeled with different dyes and electrophoresed together in the same capillary. In this way, we eliminated from consideration both capillary-to-capillary migration-rate variations and batch-to-batch matrix variability. Small thermal gradients and inconsistencies in the capillary wall coatings used to suppress the electroendosmotic flow (17,18) induce up to 10% variation in the measured retention times of DNA fragments across the capillary array. In addition, small changes in measured retention times from one electrophoretic experiment to the next occur because of slight variability between preparations of the HEC sieving medium.

The fluorescence emissions of CY5 derivatives (~665 nm) and CY5.5s (~680 nm) can be distinguished easily using the two-color detection of our CAE instrumentation (10,11). The CY5- or SQ5-labeled fragments were co-run with CY5.5-labeled fragments, for a total of 128 pairwise comparisons. The entire sequencing traces for the end-labeled M13mp18 sequencing fragments, created by ddT termination reactions, were evaluated, from primer peaks through to the onset of biased reptation (~700 bp), to determine the full relative mobility pattern of the two fragment sets. We have assumed that the dye-induced mobility behavior of the ddT terminated fragments will be conserved for ddC, ddA and ddG fragments in a full four-color sequencing experiment.

The electrophoretic mobility (µ) of each DNA fragment during capillary electrophoresis is given by $\mu = q/f$, where q is the effective charge of the fragment and f is the frictional force on the molecule migrating through the sieving medium (19). Both q and f of a DNA fragment are influenced by the attached fluorescent dye. The structure of the dye determines both the overall magnitude of the influence and what changes, if any, occur with increasing length of the fragments. Thus, paired series of fragments labeled with different dyes can show complex relative migration patterns.

Figures 2–4 show examples of three typical relative migration patterns. In Figure 2, portions of the traces for Cy5T7- and Cy5.5T5-labeled ddT termination reactions appear. For this pair, the Cy5T7-labeled fragments, with a –2 charge on the dye, migrate faster in the beginning of the run than the Cy5.5T5-labeled fragments (–1 dye charge). The relative mobility shift decreases monotonically over the first 300 bp, then the two sets of fragments co-migrate for the rest of the run. Figure 3 shows two dyes, Sq5T4 (neutral charge) and Cy5.5T12 (–2 charge), that exhibit a mobility shift crossover. The Cy5.5T12-labeled fragments initially migrate faster than Sq5T4-labeled DNA, up to ~125 bp; the order then reverses for larger fragments. In Figure 4, fragments labeled with the two dyes Cy5 and Cy5.5T5, both of which bear a –1 charge, exhibit a complete mobility match. Here, the peaks overlap perfectly throughout the entire run, within the temporal resolution of the instrumentation. Figures 2–4 illustrate the importance of using an entire sequencing ladder to evaluate the effects of the fluorescent label on the DNA migration behavior.

The results from all 128 pairwise combinations of the dye-labeled sequencing reactions are summarized in Table 1. Each position in the table indicates the relative electrophoretic migration for that dye combination (F, CY5/SQ5 dye faster than CY5.5 dye; S, CY5/SQ5 dye slower than CY5.5 dye; C, mobility crossover; M, mobility match). Using the table, comparison of two CY5 or SQ5 derivatives against all CY5.5 derivatives can be made by scanning the data across the two rows. The relative migration rates for DNA labeled with the two CY5/SQ5 dyes can then be indirectly inferred. Conversely, two CY5.5 derivatives can be compared by scanning down the appropriate columns. In this way, a relative electrophoretic mobility scale for the dyes within each dye subset (CY5s, SQ5s, CY5.5s) was generated (Fig. 5). Although this electrophoretic scale appears to randomly interweave dyes that vary by charge and structure, a careful dissection of the results yields several general principles of dye–DNA fragment mobility. Furthermore, the exceptions to these rules reveal interesting aspects of the structures of specific dye–DNA conjugates.

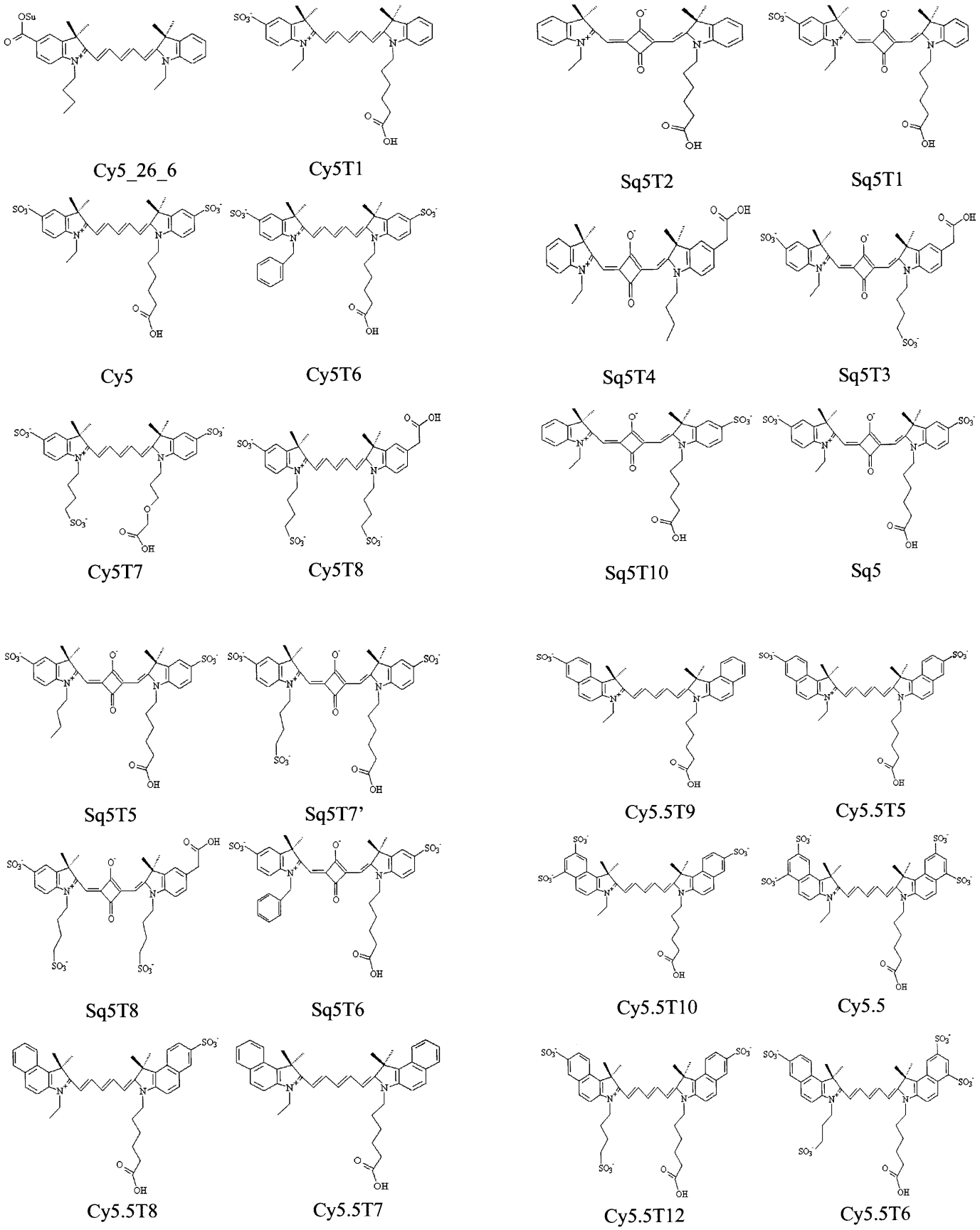

Figure 1. List of the dye structures and nomenclature used in this study.

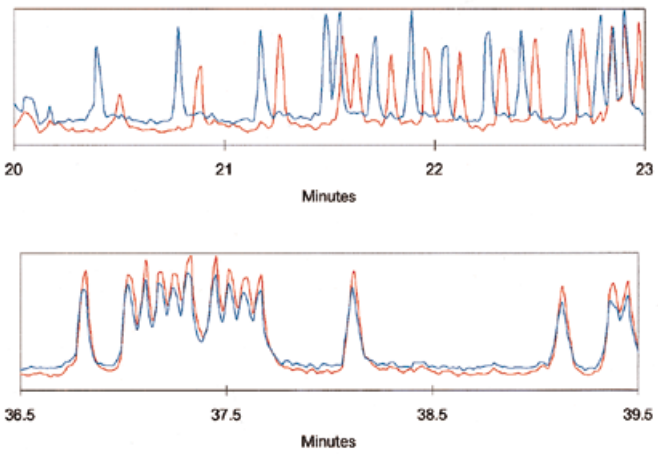

Figure 2. Electrophoretic traces for Cy5T7 and Cy5.5T5, showing the relative mobilities early in the run and in the middle of the run. Samples: M13mp18 T-termination reactions. Electrophoresis: 185 V/cm. Blue trace, Cy5T7; red trace, Cy5.5T5.

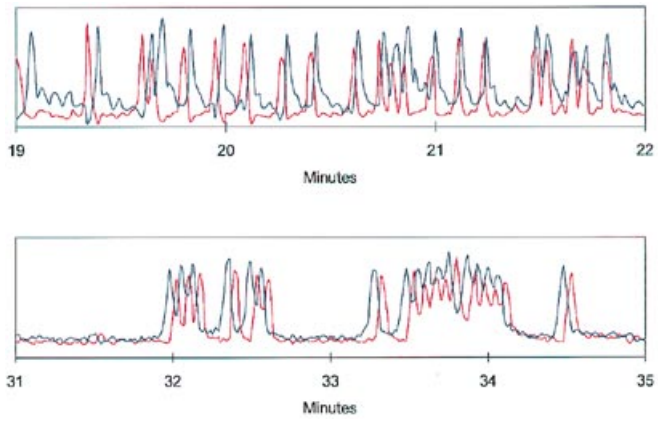

Figure 3. Electrophoretic traces for Sq5T4 and Cy5.5T12, showing the relative mobilities early in the run and in the middle of the run. Samples: M13mp18 T-termination reactions. Electrophoresis: 185 V/cm. Blue trace, Sq5T4; red trace, Cy5.5T12.

Net dye charge and dye–DNA interactions

Among the interesting features of Figure 5 is the predominance of the charge on the fluorescent dye as the main determinant of DNA mobility. Thus Cy5.5T5^{-1} < (Cy5.5T12^{-2}, Cy5.5T10^{-2}) < (Cy5.5T6^{-3}, Cy5.5^{-3}); Cy5T1^{0} < (Cy5^{-1}, Cy5T6^{-1}) < (Cy5T8^{-2}, Cy5T7^{-2}); and (Sq5T4^{0}, Sq5T2^{0}) < (Sq5T1^{-1}, Sq5T10^{-1}) ≈ (Sq5^{-2}, Sq5T5^{-2}, Sq5T6^{-2}) < (Sq5T8^{-3}, Sq5T7′$^{-3}$) (superscript indicates charge). Three exceptions to this general rule were observed. The first two are discussed in this section. The third exception, Sq5T3, is discussed in a later section on Dye–DNA linkage.

In the first exception, the neutral CY5.5 derivatives (Cy5.5T9 and Cy5.5T8) migrate anomalously fast, as though they bore a net –2 charge. This behavior is probably due to dye–DNA base interactions mediated by the ring structure present in the Cy5.5 derivatives (Fig. 1). Neutral CY5 dyes, which lack the extended ring structure present in the CY5.5s, did not exhibit this anomalous migration phenomenon. The proposed hydrophobic dye–DNA interactions may be akin to the base-stacking observed within a DNA strand or intercalation of small molecules between DNA bases (20–23).

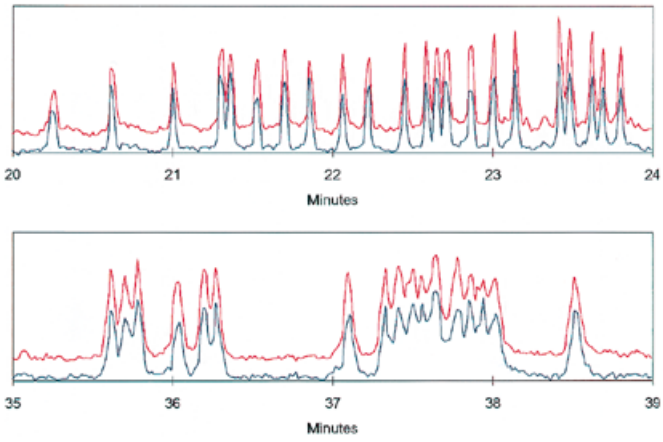

Figure 4. Electrophoretic traces for Cy5 and Cy5.5T5, showing the relative mobilities early in the run and in the middle of the run. Samples: M13mp18 T-termination reactions. Electrophoresis: 185 V/cm. Blue trace, Cy5; red trace, Cy5.5T5.

Table 1. Summary of the relative mobility shifts between dye pairs

	Cy5.5T7 +1	Cy5.5T8 0	Cy5.5T9 0	Cy5.5T5 -1	Cy5.5T10 -2	Cy5.5T12 -2	Cy5.5 -3	Cy5.5T6 -3
Cy5_26_6 +1	S	s	M	f	C	f	Cs	C
Cy5T1 0	S	s	s	s	S	s	S	S
Cy5 -1	S	s	s	M	S	s	S	S
Cy5T6 -1	S	s	s	M	s	Cm	S	S
Cy5T7 -2	Cs	C	C	f	s	f	s	s
Cy5T8 -2	Cs	s	s	f	s	f	S	S
Sq5T2 0	s	s	M	f	s	f	s	s
Sq5T4 0	S	S	s	f	s	C	S	S
Sq5T1 -1	C	F	F	f	m	f	S	s
Sq5T10 -1	C	f	f	f	f	F	s	C
Sq5T3 -2	S	S	S	s	S	s	S	S
Sq5 -2	Cs	Cm	C	f	M	f	s	s
Sq5T5 -2	C	f	f	F	m	f	s	m
Sq5T6 -2	C	f	f	f	f	f	s	s
Sq5T7' -3	f	f	F	F	F	F	Cm	f
Sq5T8 -3	C	f	F	F	f	F	s	f

Score indicates which dye of the pair migrates faster: **f**, CY5/SQ5 derivative faster; **F**, CY5/SQ5 derivative much faster; **s**, CY5/SQ5 derivative slower; **S**, CY5/SQ5 derivative much slower; **m**, near mobility match (peak separations ≤0.2 peak FWHM); **M**, identical mobility match (peaks coincident); **C**, mobility crossover; **Cm**, near mobility match, but with a small mobility crossover; **Cs**, mobility crossover, but with CY5/SQ5 derivative predominantly slower.

These interactions would result in loop or hairpin structures on the 5′ terminus of the DNA fragments. Such structures would induce a faster migration rate for the DNA relative to the more extended structures adopted by most dye–DNA conjugates involving

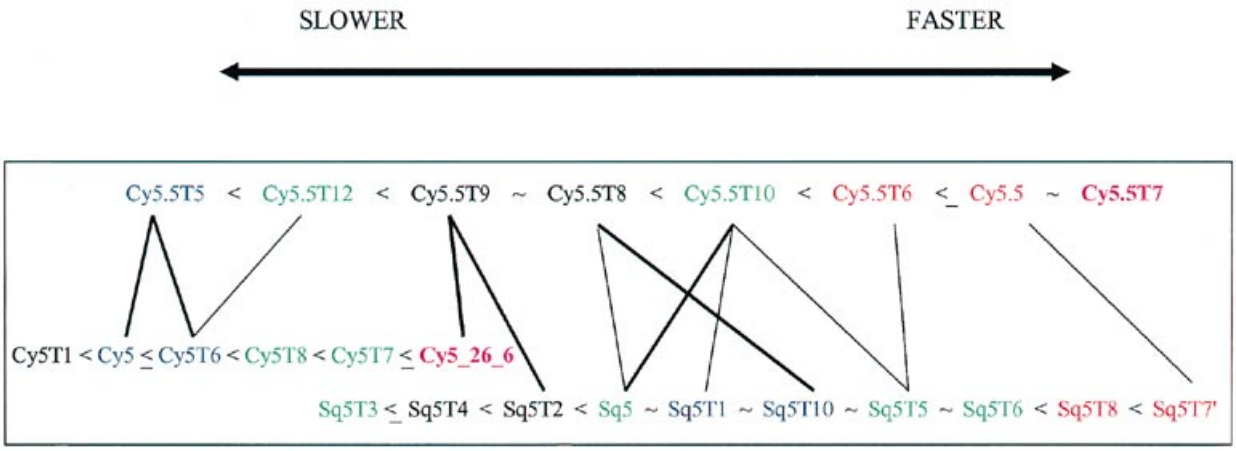

Figure 5. Relative electrophoretic velocity scale for the subsets of dye families. Lines connecting the dyes indicate mobility matches. Thick lines indicate identical matches, and narrow lines indicate nearly perfect matches. Colors correspond to the net charge on the dyes: pink, +1; black, neutral; blue, –1; green, –2; red, –3. The Cy5 and Sq5 dyes have been separated on the scale for clarity.

negatively charged dyes, just as compression artifacts in DNA sequencing data are caused by 3′ hairpin structures.

In the second exception, the positively charged Cy5_26_6 and Cy5.5T7 migrate faster than all other CY5 and CY5.5 derivatives, respectively. This is also presumably caused by dye–DNA interactions, but here the interaction is driven by electrostatic attraction (Cy5_26_6) or by both electrostatic and hydrophobic forces (Cy5.5T7) (22,23). Here again, the resultant hairpin structures would induce a faster migration rate for the labeled DNA fragments.

Charge location and organic groups

A closer examination of both the CY5 and the SQ5 dyes reveals that the position of peripheral charges on the dye molecules also has an influence on dye mobility. Charged sulfonate groups placed directly on the dye ring structures increase the mobility more than similar charges placed off the heterocyclic nitrogen position. For example, $Cy5.5T10^{-2}$ migrates faster than $Cy5.5T12^{-2}$, and $Cy5.5^{-3}$ is slightly faster than $Cy5.5T6^{-3}$. In contrast, the results for $Cy5.5T8^{0} \approx Cy5.5T9^{0}$ and $Sq5T10^{-1} \approx Sq5T1^{-1}$ indicate that it is not particularly important which ring carries the charge.

Unlike charged groups, peripheral organic groups from one of the heterocyclic nitrogens exert a negligible influence on DNA mobility. Thus, Cy5T6 ≥ Cy5, and Sq5 ≈ Sq5T5 ≈ Sq5T6.

Dye–DNA linkage

The point of linkage between the dye and the DNA can have a marked influence on DNA fragment mobility. In the present series, linkage from a heterocyclic nitrogen gives rise to faster DNA migration rates than linkage from a phenyl ring. Examples of this effect include Cy5T7 > Cy5T8, Sq5T2 > Sq5T4, and Sq5T7′ > Sq5T8. Most dramatically, Sq5T3-labeled fragments migrate the slowest of all of the SQ5- or CY5-labeled DNAs.

Squarine dyes

As shown in Figure 5, the squarine dyes display a number of interesting features. Most of the SQ5s in the charge range –1 to –2 produced very similar migration rates, with both $Sq5T1^{-1}$ and $Sq5T10^{-1}$ falling between $Sq5^{-2}$ and $Sq5T5^{-2}$/$Sq5T6^{-2}$ on the velocity scale, and only very small differences in mobility profiles across this entire group. Note that in the pairwise data $Cy5.5T10^{-2}$ mobility matches $Sq5^{-2}$, $Sq5T1^{-1}$ and $Sq5T5^{-2}$. All of the SQ5 derivatives, except for Sq5T3 (see previous section), migrate significantly faster than the charge-matched CY5 derivatives. The placement of a negative charge in the middle of the SQ5 molecules, as opposed to the periphery of the ring structures, may decrease the extent of dye solvation, and hence increase the effective net charge of the SQ5 dyes relative to the Cy5′s within the buffered electrophoretic medium. The SQ5 dyes, however, are expected to be much more conformationally rigid than the CY5 dyes due to their central ring structure, and this should increase the frictional drag experienced by these dyes during electrophoresis relative to the CY5 dyes. In this model, the influences of charge and frictional drag would work against each other, but the combined effects of charge solvation and structural rigidity are worth ~1–2 charge units relative to the CY5 dyes: $Sq5T4^{0} \geq Cy5T6^{-1}$; $Sq5T2^{0} > Cy5T7^{-2}$.

The neutral Sq5T4 and Sq5T2 migrate much faster than Sq5T3 (–2 charge). This result was described above in relation to the slow migration of Sq5T3 due to its dye–DNA linkage mode, but the result may also be due in part to an enhanced migration rate for the neutral SQ5 derivatives.

The results are consistent with both the neutral and –1-charged SQ5 dyes being able to adopt dye–DNA conjugate secondary structures that enhance the fragment mobilities. The nature of these structures and interactions are unclear, but these are the only results not easily interpretable within the framework of the general rules described here. Further experiments are necessary to more clearly delineate the structures of these dye–DNA constructs.

Electrophoresis conditions

We investigated the temperature dependence of the relative mobility profiles by raising the electrophoresis temperature from 28°C to 34 and 42°C and retesting the dye pairs that, in Figure 5, showed close or identical mobility matches. Of the five pairs showing identical migration patterns, all remained identically matched at the higher temperatures. The three near-match pairs with one member slightly faster than the other, and two of the three near matches with crossover at 28°C continued to provide near matches at 34 and 42°C. Thus, the majority of matched pairs were good matches over a wide range of run temperatures,

implying that any dye–DNA interactions present in these conjugates are generally stable over the tested temperature range. Only the Cy5.5T8-Sq5 pair changed from a near match with a small crossover to a poor match with a marked mobility crossover at the higher temperatures.

The dependence of matched mobilities on the HEC concentration was examined by testing the dye pairs that remained close or identical matches at elevated temperatures in both 1.5 and 1.25% HEC solutions at 35°C. The mobilities remained matched at both HEC concentrations.

CONCLUSIONS

This study represents the first attempt to systematically correlate dye structure with the electrophoretic mobilities of labeled DNA fragments. As expected for this set of structurally similar dyes, the relative charges on different dyes is a gross determiner of relative DNA mobility. In addition, interactions between the dyes and the DNA can, in some cases, play a major role in determining mobility by changing the translational friction coefficients for the DNA fragments through the sieving medium. DNA electrophoretic mobility can in fact be used as a diagnostic for such interactions. Both electrostatic and hydrophobic forces may be important for inducing this phenomenon, and, as found with other ligands (20,22), the presence of extended ring structures on the dyes may influence the proposed hydrophobic interactions. It is also apparent that subtle changes in dye structure, such as the location of a charge within a molecule, can provide the effects needed to generate mobility-matched sets of dye-labeled DNA sequencing primers. By examining a structurally similar series of dyes, we were able to identify a number of mobility-matched dye pairs for use in DNA sequencing and fragment sizing applications.

ACKNOWLEDGEMENTS

The authors wish to thank Dr Richard Mathies and Dr James K. Bashkin for helpful discussions.

REFERENCES

1 Kricka, L. J. (1992) *Nonisotopic DNA Probe Techniques*. Academic Press, San Diego, CA.
2 Smith, L. M., Sanders, J. Z., Kaiser, R. J., Hughes, P., Dodd, C., Connell, C. R., Heiner, C., Kent, S. B. H. and Hood, L. E. (1986) *Nature*, **321**, 674–679.
3 Ju, J., Ruan, C., Fuller, C. W., Glazer, A. N. and Mathies, R. A. (1995) *Proc. Natl. Acad. Sci. USA*, **92**, 4347–4351.
4 Ju, J., Kheterpal, I., Scherer, J. R., Ruan, C., Fuller, C. W., Glazer, A. N. and Mathies, R. A. (1995) *Anal. Biochem*., **231**, 131–140.
5 Ju, J., Glazer, A. N. and Mathies, R. A. (1996) *Nucleic Acids Res*., **24**, 1144–1148.
6 Metzker, M. L., Lu, J. and Gibbs, R. A. (1996) *Science*, **271**, 1420–1422.
7 Hung, S. C., Ju, J., Mathies, R. A. and Glazer, A. N. (1996) *Anal. Biochem*., **243**, 15–27.
8 Hung, S. C., Mathies, R. A. and Glazer, A. N. (1997) *Anal. Biochem*., **252**, 78–88.
9 Middendorf, L. R., Bruce, J. C., Bruce, R. C., Eckles, R. D., Grone, D. L., Roemer, S. C., Sloniker, G. D., Steffens, D. L., Sutter, S. L., Brumbaugh, J. A. and Patonay, G. (1992) *Electrophoresis*, **13**, 487–494.
10 Bashkin, J. S., Bartosiewicz, M., Roach, D., Leong, J., Barker, D. and Johnston, R. (1996) *J. Capillary Electrophoresis*, **3**, 1–15.
11 Bashkin, J. S., Marsh, M., Barker, D. and Johnston, R. (1996) *Appl. Theor. Electrophoresis*, **6**, 23–28.
12 Marsh, M., Tu, O., Dolnik, V., Roach, D., Solomon, N., Bechtol, K., Smietana, P., Wang, L., Li, X., Cartwright, P., Marks, A., Barker, D., Harris, D. and Bashkin, J. (1997) *J. Capillary Electrophoresis*, **4**, 83–89.
13 Ernst, L. A., Gupta, R. K., Mujumdar, R. B. and Waggoner, A. S. (1989) *Cytometry*, **10**, 3–10.
14 Mujumdar, R. B., Ernst, L. A., Mujumdar, S. R. and Waggoner, A. S. (1989) *Cytometry*, **10**, 11–19.
15 Southwick, P. L., Ernst, L. A., Tauriello, E. W., Parker, S. R., Mujumdar, R. B., Mujumdar, S. R., Clever, H. A. and Waggoner, A. S. (1990) *Cytometry*, **11**, 418–430.
16 Mujumdar, R. B., Ernst, L. A., Mujumdar, S. R., Lewis, C. J. and Waggoner, A. S. (1993) *Bioconjugate Chem*., **4**, 105–111.
17 Hjertén, S. (1985) *J. Chromatog*., **347**, 191–198.
18 Cobb, K. A., Dolnik, V. and Novotny, M. (1990) *Anal. Chem*., **62**, 2478–2483.
19 Weinberger, R. (1993) *Practical Capillary Electrophoresis*, Academic Press, San Diego, CA.
20 Sammes, P. G. and Yohioglu, G. (1994) *Chem. Soc. Reviews*, **23**, 327–334.
21 Asseline, U., Bonfils, E., Dupret, D. and Thuong, N. T. (1996) *Bioconjugate Chem*., **7**, 369–379.
22 Satyanarayana, S., Dabrowiak, J. C. and Chaires, J. B. (1992) *Biochemistry*, **31**, 9319–9324.
23 Bustamante, C. and Stigter, D. (1984) *Biopolymers*, **23**, 629–645.